The Astrophysical Journal, 571:771–778, 2002 June 1

THE HELLAS2*XMM* SURVEY. II. MULTIWAVELENGTH OBSERVATIONS OF P3: AN X-RAY–BRIGHT, OPTICALLY INACTIVE GALAXY[1]

A. Comastri, M. Mignoli, and P. Ciliegi
Osservatorio Astronomico di Bologna, via Ranzani 1, I-40127 Bologna, Italy; comastri@bo.astro.it, mignoli@bo.astro.it, ciliegi@bo.astro.it

P. Severgnini
Dipartimento di Astronomia e Scienze dello Spazio, Largo E. Fermi 5, I-50125 Florence, Italy; paolas@arcetri.astro.it

R. Maiolino
Osservatorio Astrofisico di Arcetri, Largo E. Fermi 5, I-50125 Florence, Italy; maiolino@arcetri.astro.it

M. Brusa
Dipartimento di Astronomia Universita' di Bologna, via Ranzani 1, I-40127 Bologna, Italy; brusa@bo.astro.it

F. Fiore
Osservatorio Astronomico di Roma, via Frascati 33, I-00040 Monteporzio, Italy; fiore@quasar.mporzio.astro.it

A. Baldi and S. Molendi
Istituto di Fisica Cosmica, CNR, via Bassini 15, I-20121 Milan, Italy; baldi@ifctr.mi.cnr.it, silvano@ifctr.mi.cnr.it

R. Morganti
Netherlands Foundation for Research in Astronomy, Postbus 2, 7990 AA Dwingeloo, The Netherlands; morganti@nfra.nl

C. Vignali
Department of Astronomy and Astrophysics, Pennsylvania State University, 525 Davey Lab, University Park, PA 16802; chris@astro.psu.edu

and

F. La Franca, G. Matt, and G. C. Perola
Dipartimento di Fisica Universita' di Roma Tre, via della Vasca Navale 84, I-00146 Rome, Italy;
matt@fis.uniroma3.it, lafranca@fis.uniroma3.it, perola@fis.uniroma3.it
Received 2001 December 14; accepted 2002 February 4

ABSTRACT

Recent X-ray surveys have clearly demonstrated that a population of optically dull, X-ray–bright galaxies is emerging at 2–10 keV fluxes of the order of 10^{-14} ergs cm^{-2} s^{-1}. Although they might constitute an important fraction of the sources responsible for the hard X-ray background, their nature is still unknown. With the aim of better understanding the physical mechanisms responsible for the observed properties, we have started an extensive program of multiwavelength follow-up observations of hard X-ray, optically quiet galaxies discovered with *XMM-Newton*. Here we report the results of what can be considered the first example of this class of objects: CXOU J031238.9−765134, originally discovered by *Chandra*, and optically identified by Fiore et al. (2000) with an apparently normal early-type galaxy at $z = 0.159$, usually known as FIORE P3. Analysis of the broadband energy distribution suggests the presence of a heavily obscured active nucleus.

Subject headings: galaxies: active — galaxies: individual (P3) — galaxies: nuclei — X-rays: galaxies

1. INTRODUCTION

The discrete sources responsible for a large fraction (>75 %) of the X-ray background emission below 8 keV have been detected by *Chandra* deep surveys down to extremely faint fluxes $S_{2-8\,\mathrm{keV}} < 10^{-15}$ ergs cm^{-2} s^{-1} (Mushotzky et al. 2000; Giacconi et al. 2001; Hornschmeier et al. 2001; Brandt et al. 2001; Tozzi et al. 2001). The unprecedented arcsec *Chandra* spatial resolution allows us to unambiguously identify the optical counterparts of the X-ray sources. Extensive programs of optical identification showed that about half of them are associated with optically bright objects at redshifts <1.5, while the other half appears to be a mixture of optically faint ($I > 23.5$) galaxies and active galactic nuclei (AGNs), presumably at high redshift. The source breakdown of the optically bright population is intriguing. Contrary to the situation for the faint soft X-ray–selected *ROSAT* sources (Schmidt et al. 1998), only a minority (<20%) of them are associated with broad line objects and, even more surprisingly, some 50% of the spectroscopically identified sources do not show obvious signatures of AGN activity in their optical spectra, which are instead typical of early-type "normal" galaxies (Hornschemeier et al. 2001; Giacconi et al. 2001; Barger et al. 2001). These findings seem to support previous claims (Griffiths et al. 1995) based on lower spatial resolution *ROSAT* observations.

The large X-ray–to–optical flux ratio, which exceeds by more than 1 order of magnitude the average value of early-type galaxies of similar optical luminosity (Fabbiano, Kim, & Trinchieri 1992), and the hard X-ray spectra, determined from the analysis of X-ray colors, both suggest that (obscured) AGN activity is taking place in their nuclei. In principle, X-ray spectroscopy could provide a stringent test

[1] This work is based on observations collected at the European Southern Observatory (proposal 66.B-0472A), La Silla and Paranal, Chile, and observations made with the *XMM-Newton*, an ESA science mission with instruments and contributions directly funded by ESA member states and the USA (NASA).

of their nature. Unfortunately, all the sources are detected with a number of photons that is too small to apply conventional X-ray spectral fitting techniques to and to constrain the absorbing column density. The lack of optical emission lines could also be explained if the nuclear light is overshined by either the stellar continuum or a nonthermal component, or if they are not efficiently produced.

A much better understanding of the sources powering X-ray–bright, optically quiet galaxies can be achieved only by means of multiwavelength observations. For this reason, we have started an extensive program of multifrequency follow-up observations of hard X-ray–selected sources serendipitously discovered in *XMM-Newton* fields over an area of about 3 deg^2 (the *XMM* High Energy Large Area Survey HELLAS2*XMM*; see Baldi et al. 2002).

In this paper, we present a multiwavelength study of what can be considered the first example of these objects: the X-ray source CXOU J031238.9−765134, optically identified as a bright ($R = 18.0$), "normal" early-type galaxy at $z = 0.159$ by Fiore et al. (2000, hereafter F00) in their pilot study of serendipitous X-ray sources in two shallow *Chandra* fields.

2. OBSERVATIONS

The field surrounding the radio-loud quasar PKS 0312−76 has been observed by both *Chandra* and *XMM-Newton* during their calibration and performance phases. The *Chandra* source CXOU J031238.9−765134 (hereafter P3, being the third source cataloged by F00 in the PKS field), was also detected by *XMM* with a number of photons sufficient for a rough spectral analysis. Here we present the X-ray spectral analysis combined with deep radio observations and near-infrared and optical spectroscopy.

2.1. *X-Ray Data*

The analysis of *Chandra* data, based on preliminary calibration data and detection techniques, has already been reported by F00. An additional observation of the PKS 0312−76 field was retrieved from the archive, combined with the first one, and analyzed using version 2.2 of the CXC software. The periods of high background were filtered out, leaving about 24.7 ks of useful data. The WAVDETECT algorithm (Freeman et al. 2002) was run on the cleaned image, conservatively setting the false-positive probability threshold to 10^{-7}. The source was clearly detected in both the soft (0.5–2 keV) and hard (2–8 keV) bands with 40 ± 6 and 22 ± 5 net counts, respectively. Although the counting statistics do not allow a proper spectral analysis, the hard-to-soft band ratio of 0.55 ± 0.15 implies a hard power-law spectrum ($\Gamma \simeq 1.4$), assuming the Galactic absorption column density ($N_{\rm H} = 8 \times 10^{20}$ cm^{-2}; Dickey & Lockman 1990). The 2–10 keV *Chandra* flux is 2.5×10^{-14} ergs cm^{-2} s^{-1}, consistent with that reported by F00.

Our target was also clearly detected in the 25 ks *XMM–Newton* PV observation of the same field. Even though the *XMM* positional accuracy is not as good as the *Chandra* one, the two X-ray centroids agree within about 2″. The *XMM* and *Chandra* contours are overlaid on an *R*-band optical image in Figure 1. It can be seen that the elongated *XMM* contours are probably due to the presence of a faint X-ray source which is clearly resolved by *Chandra* at a distance of ∼6″ from P3. This object appears to be coincident with an extremely faint $R > 24$ optical counterpart. Its X-ray flux is only about 10%–15% of P3, while its hardness ratio suggests a spectral shape similar to P3.

The *XMM* data were processed using version 5.0 of the Science Analysis System (SAS). The event files were cleaned up from hot pixels and soft proton flares (see Baldi et al. 2002 for details). The hot pixels were removed using both the *XMM*-SAS and the IRAF task COSMICRAYS, while for the proton flares, a count rate threshold was applied removing all the time intervals with a count rate greater than 0.15 counts per second in the 10–12.4 keV energy range for the two MOS and greater than 0.35 counts per second in the 10–13 keV band for the *p-n* unit. The resulting exposure times are 24.7, 26.5, and 26.1 ks in the *p-n*, MOS1, and MOS2 detectors, respectively. The source is clearly detected in both the soft (0.5–2 keV) and hard (2–10 keV) bands with an approximately equal number of net counts (about 100 for each band combining the *p-n* and MOS data). Source and background spectra were extracted from the cleaned events using an extraction radius of about 26″ for the *p-n*, 35″ for MOS1 and 17″ for MOS2 (the source is near a CCD gap). Background spectra were extracted by nearby source-free regions with radii between 1′ and 1.′5, depending on the detector. The PN and MOS spectra were rebinned with at least 20 counts per channel and fitted simultaneously using XSPEC 11.0, leaving the relative normalizations free to vary. The latest version of response and effective area files was used. The Galactic column density in the direction of P3 is included in the spectral fits. The limited counting statistics of the observed spectra allow us to fit only simple models. Acceptable fits are obtained with both a power law with photon index $\Gamma = 1.10 \pm 0.35$ and with a thermal model with an extremely high temperature $kT > 9$ keV, confirming the presence of the hard spectrum inferred from the *Chandra* hardness ratio. A good description of the data is also obtained fixing the power-law slope at $\Gamma = 1.8$ (an average value for AGNs; e.g., Nandra et al. 1997): this gives an absorption column density $N_{\rm H} = 8 \pm 5 \times 10^{21}$ cm^{-2} at the source frame (errors are at the 90% confidence level for one parameter). The 2–10 keV flux is in the range 2.5–3.0 $\times 10^{-14}$ ergs s^{-1} cm^{-2}, depending on the *XMM* detector, and is in good agreement with the *Chandra* value. The absorption-corrected 2–10 keV luminosity is about 3×10^{42} ergs s^{-1}. The good agreement between the power-law slope and the hard X-ray flux measured by *Chandra* and the *XMM-Newton* suggests the lack of significant flux and spectral variability on a timescale of about 7 months. Taking into account the present uncertainties in the adopted spectral models and the *Chandra* versus *XMM-Newton* cross-calibrations (Snowden 2002), the maximum fractional variability allowed by the data is of the order of 30%. Our results are in good agreement with those recently obtained by Lumb, Guainazzi, & Gondoin (2001) from the analysis of the same *XMM-Newton* data. Our analysis, however, relies on a more detailed evaluation of the instrumental and cosmic backgrounds at the source position.

2.2. *The Optical Spectrum*

The spectroscopic observations have been performed with the ESO 3.6 m telescope equipped with EFOSC2 (Patat 1999) during two different observing runs. On the night of 2000 January 4, we used the grism 6 and a slit width of 2″,

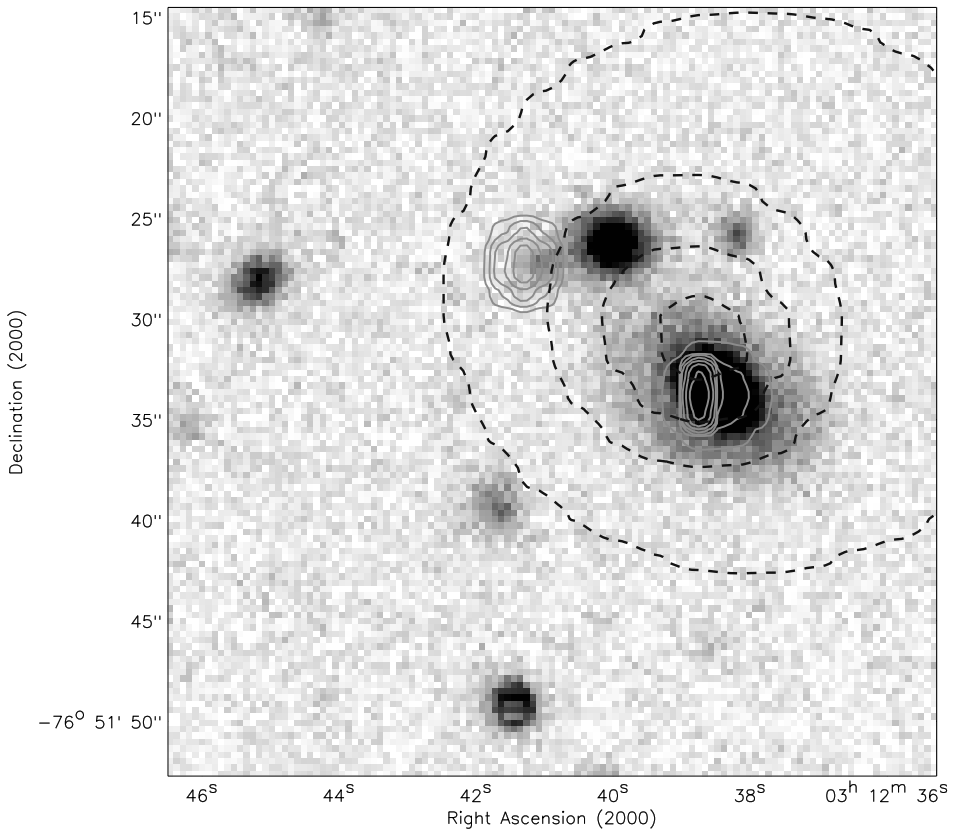

FIG. 1.—*Chandra* (*solid line*) and *XMM-Newton* (*dashed line*) contours overlaid on the *R*-band image. P3 is the galaxy coincident with the southern *Chandra* source.

whereas the grism 13 with a 1.″5 slit was used on the night of 2000 December 26. Both configurations[2] yield a similar resolution of about 26 Å, but with the latter setup, the spectrum extends more toward the red up to 9000 Å. The spectroscopic data have been reduced separately using standard IRAF routines. Bias exposures taken on each night were stacked, checked for consistency with the overscan regions of spectroscopic frames, and subtracted out. The bias-subtracted frames were then flat-fielded in a standard manner using internal lamp flats obtained during the same run. The sky background was removed by fitting a third-order polynomial along the spatial direction in source-free regions. The two-dimensional spectra of P3 have been checked by eye and extracted via optimal averaging (Horne 1986). In both the observing runs, the wavelength calibration was made using the HeAr arc lamp and using the spectroscopic standard star LTT 4364 (Hamuy et al. 1994) for flux calibration. The slit was oriented with different position angles during the two observations; in one case, we set the angle in order to include in the slit both the principal target and a nearby fainter object (which turned out to be a background galaxy). The other position angle has been chosen to include a bright star in the slit in order to perform an optimal subtraction of the atmospheric telluric features. Due to the different slit orientations, the nonphotometric conditions of the nights, and the relatively narrow slits we used, the present spectra cannot be considered spectrophotometric. The comparison of spectra taken 1 yr apart shows good agreement, compatible with the precision of the flux calibration (∼15%). In Figure 2, we show the average of the two spectra with the principal identified absorption lines labeled. We also mark the [O II] emission line at 3727 Å and the expected position of the Hα features. Unfortunately, at the redshift of P3, the Hα line position coincides with the strongest atmospheric telluric band in the optical. We did our best to remove the telluric features, but we cannot absolutely exclude the presence of a weak feature, either in emission or in absorption.

The average redshift is $z = 0.1595 \pm 0.0007$, measured from the position of the principal absorption lines and by cross-correlation with an early-type galaxy template.

2.3. *The Near-Infrared Spectrum*

Near-infrared spectroscopic observations of the P3 galaxy were performed at the ESO Very Large Telescope (VLT). The data were collected on 2000 November 10 and 11 under good seeing (0.″7–0.″9) and photometric conditions. The galaxy has been observed with the 1″ slit in two different filters, *SH* (1.42–1.83 μm) and SK (1.84–2.56 μm), available for the low resolution grating (LR) in the short wavelength (SW) configuration of ISAAC (Moorwood et al. 1999).[3] The pixel size is 0.″147 per pixel along the slit, and the resolving powers were 500 and 450 in the *SH* and *SK*

[2] For more information, see http://www.ls.eso.org/lasilla/Telescopes/360cat/efosc/docs/Efosc2Grisms.html.

[3] See http://www.hq.eso.org/instruments/isaac for more information.

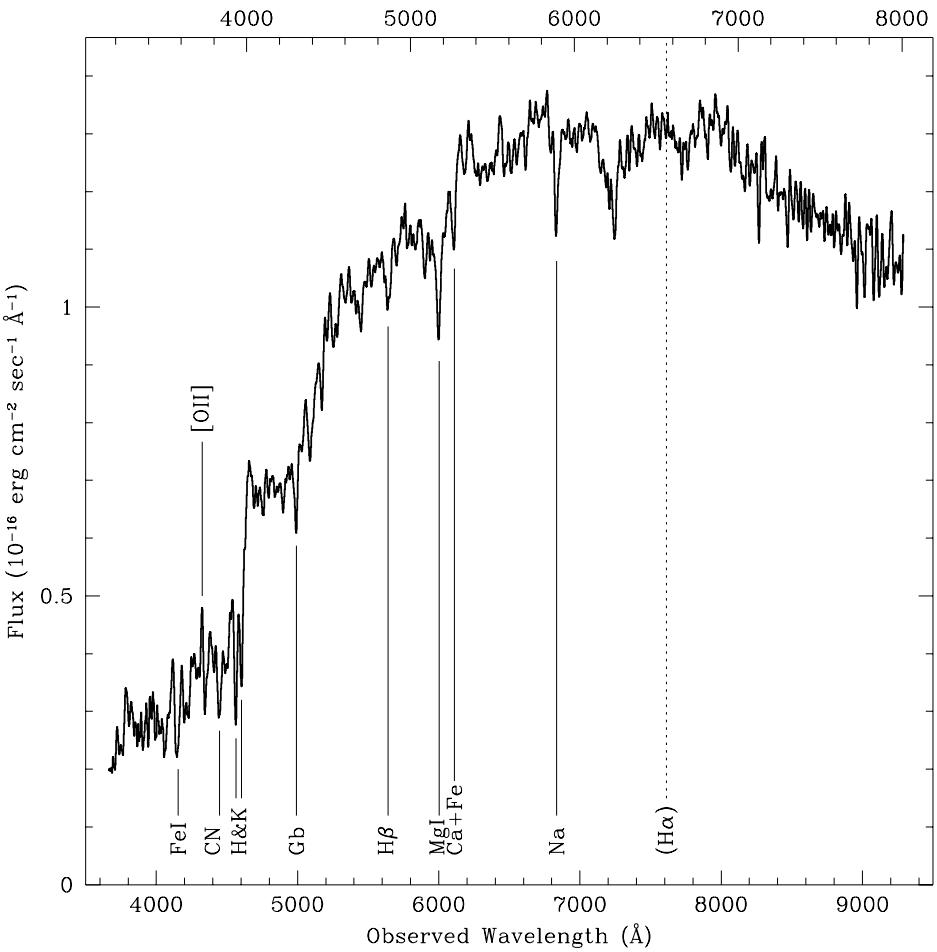

FIG. 2.—Flux-calibrated co-added optical spectrum. Spectral features are indicated with solid lines, while the dotted line is at the wavelength corresponding to Hα.

bands, respectively. The target was observed several times at different positions along the slit (nodding mode). Each single exposure was 200 s long, resulting in a total exposure time of 2 hr in each filter. The data were reduced using routines from the ECLIPSE (Devillard 1998), IRAF, and MIDAS packages. Since we observed in nodding mode, the dark, bias, and sky contributions were removed by subtracting the pairs of offset frames. The data were then flat-fielded using a master flat-field image. Wavelength calibration and correction for distortions along the slit were performed using ArXe arc exposures, while the distortion along the spatial direction was corrected using the star-trace exposures provided by ESO. The individual frames were then aligned and combined. The telluric absorption features were removed using the spectroscopic standard Hip 33590 (A0 V) after deleting from the standard spectrum the intrinsic stellar features. To obtain the intrinsic shape of the continuum of the galaxy and to perform the flux calibration, we have used a blackbody curve with the appropriate temperature to fit the intrinsic continuum of the standard. In order to correct for the slit losses, we have finally normalized the spectra to the magnitudes in the H and K_s bands ($H = 15.7$, $K = 14.9$) obtained by the acquisition images. The final spectra in both the *SH* and *SK* filters are shown in Figure 3. The infrared spectrum is consistent, within the precision of the flux calibration ($\sim$15%), with a featureless continuum. There is no evidence of significant emission lines and, in particular, of Pα.

Imaging observations in the L band (3.8 μm) have been performed at the VLT with the ISAAC camera along with the NIR spectroscopy. About half of the total exposure time of 30 minutes was lost due to technical problems. The images have been acquired combining chopping and telescope nodding in opposite directions to allow a better sky subtraction (see ISAAC User Manual). All of the chopped images, i.e., background-subtracted frames with a positive and negative image, have been flat-fielded and then combined together with a median filter to obtain the final image. The data have been calibrated using the IR photometric standard HD 219761 from the Van der Bliek, Manfroid, & Bouchet (1996) list. The source is not detected at the limiting magnitude $L = 13.4$ (3 σ upper limit).

2.4. *Radio Data*

Radio observations of the PKS 0312−76 field were performed at 5 GHz with the Australia Telescope Compact Array (ATCA) in the 6 km configuration (maximum baseline length), with a resolution of 2×2 arcsec^2. The data were collected in a run of 12 hr on 2000 September 27. In order to improve the sensitivity by a factor of $2^{1/2}$, we used both ATCA receivers at 5000 MHz, each with a bandpass of

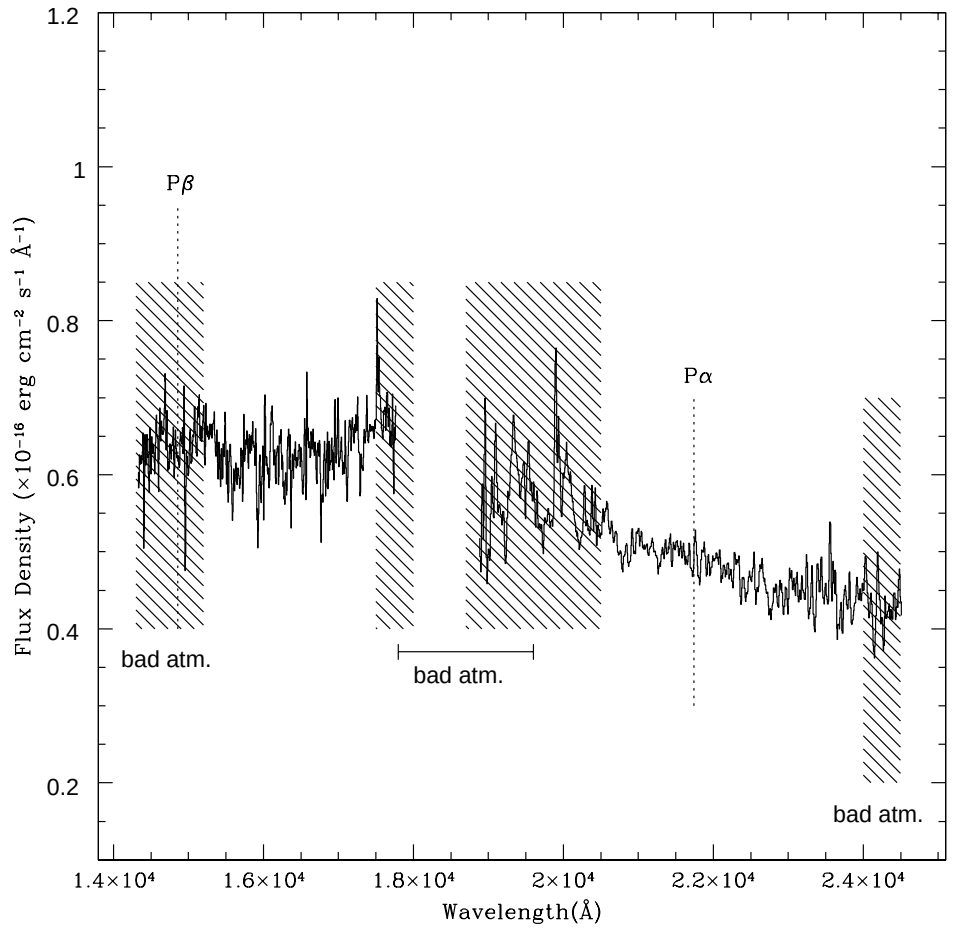

FIG. 3.—VLT ISAAC infrared spectrum. Shaded regions correspond to wavelengths of bad atmospheric transmissions. The expected positions of Pα and Pβ lines are also indicated.

128 MHz. The optimal positioning of the bands was obtained by centering one frequency at 4800 MHz (4736–4864 MHz) and the other at 5824 MHz (5760–5888 MHz). The primary flux density calibrator was PKS 1934−638, while the source PKS 0230−790 was used as a phase and secondary amplitude calibrator. The field was observed in the mosaic mode by cycling through a grid of five pointings on the sky, one of which was centered on the position of P3. The grid of the pointings in the mosaic was designed to yield uniform noise over the area covered by the *Chandra* data. With the mosaic technique, images obtained with single pointings are combined together into a large image (mosaic) of the entire observed region.

The data were analyzed with the software package MIRIAD. Each bandpass (4800 and 5824 MHz) was calibrated and cleaned separately to produce two individual images that we combined together into a single mosaic at the end of the reduction phase. Self-calibration was used to make additional correction to the antenna gains and to improve the image quality. The final map has a uniform noise of 50 μJy (1 σ) over an area with a semicircular shape (due to the odd numbers of pointings) with a radius of about 10′, surrounded by an area where the noise increases with the distance from the center.

The P3 galaxy is well inside the area with a uniform noise of 50 μJy. We searched for a possible radio source within a box of 20″ × 20″ arcsec centered on the *Chandra* position. No sources were found down to 100 μJy (2 σ). Therefore, we can conclude that the P3 galaxy does not have a radio counterpart in our map and that its 3 σ radio upper limit at 5312 MHz is 0.15 mJy.

3. DISCUSSION

Although the overall spectral energy distribution (SED) is dominated by the optical-infrared light of the host galaxy, the X-ray flux level is almost 2 orders of magnitude higher than that expected on the basis of the L_X-L_B correlation of early-type galaxies (Fabbiano et al. 1992).

The relatively high X-ray luminosity and the X-ray spectral properties strongly suggest nuclear activity in the central region of P3. Based on the *Chandra* detection and the optical spectrum F00 suggested, three different possibilities; namely, a radiatively inefficient advection dominated accretion flow (ADAF), a BL Lac object or a hidden, possibly obscured, Seyfert-like AGN. The multiwavelength observations presented in this paper allow us to investigate these possibilities in more detail.

The *ASCA* detection of relatively luminous ($L_{2-10\,\mathrm{keV}} \simeq 10^{40}$–$10^{42}$ ergs s^{-1}), extremely hard power-law components ($\langle\alpha\rangle = 0.2$) in the nuclei of six nearby elliptical galaxies that are known to host a massive black hole (Allen, Di Matteo, & Fabian 2000) was consistent, given the observed radio emission, with an ADAF model in which a significant fraction of energy is removed from the flow by winds. This possibility, however, appears to be inconsistent

with recent *Chandra* observations of three of these galaxies (Loewenstein et al. 2001): most of the spatially unresolved hard X-ray emission detected by *ASCA* originates in X-ray binaries. The lack of significant hard X-ray emission at the position of the optical nuclei allowed us to place upper limits of about 1–2 orders of magnitude lower than the luminosities estimated by Allen et al. (2000). Although ADAF models with strong outflows or convection might still be accommodated with the *Chandra* observations, the parameters computed by Allen et al. (2000) to fit the *ASCA* data need to be reconsidered. A detailed comparison of ADAF models to the present data is beyond the scope of this paper. Here we limit ourselves to compare the observed fluxes in the radio and X-ray band with the model spectra of Quataert & Narayan (1999) for several values of the physical parameters involved in the ADAF models with winds, as most of the bolometric luminosity predicted by these models is produced in the hard X-ray and radio bands. For the range of model parameters computed by Quataert & Narayan (1999), the X-ray flux density is about 1–2 orders of magnitude greater than the radio flux density (see their Fig. 7). The observed lower limit on the X-ray to radio flux density of P3 ($>10^3$) is clearly inconsistent with ADAF model predictions.

The observed SED is consistent with an early-type galaxy template normalized to match the optical and infrared spectrum plus the average SED of radio-quiet AGNs (Elvis et al. 1994) rescaled to the observed X-ray flux (Fig. 4*a*). We note that the average SED of radio-quiet quasars has been obtained from a sample of high-luminosity quasars and thus is unlikely to be appropriate for low-luminosity AGNs (LLAGNs) which are known to be characterized by a quite different broadband spectrum (Ho 1999). In particular, low-luminosity objects lack an ultraviolet excess and have a more pronounced contribution from X-rays to the overall energy output. The relative ratio between X-ray and optical flux is usually parameterized by the two-point spectral index α_{ox} (the slope obtained connecting the fluxes at 2500 Å and 2 keV), which is significantly lower for low-luminosity AGNs (between 0.5 and 1.0) with respect to higher-luminosity Seyferts and quasars, for which $\langle\alpha_{ox}\rangle \simeq 1.5$ (e.g., Brandt, Laor, & Wills 2000). The calculation of α_{ox} for P3 is not straightforward, as the 2500 Å flux density obtained extrapolating the observed optical spectrum is likely to be dominated by the host galaxy. As a consequence, the derived value of $\alpha_{ox} = 0.92$ should be considered an upper limit on the " nuclear " optical–to–X-ray flux ratio. Prompted by the similarities between LLAGN and the P3 multiwavelength data, the broadband SED of the four LLAGNs hosted by an elliptical galaxy in the Ho (1999) sample has been compared with that of P3 and normalized to the observed X-ray flux (Fig. 4*b*). Although the comparison sample is very small, we note that the average flux in the radio band of low-luminosity AGNs greatly exceeds the observed upper limit. The general trend of increasing X-ray variability for decreasing X-ray luminosities (Nandra et al. 1997) would also be inconsistent with the lack of strong X-ray variability.

The BL Lac hypothesis might be tenable despite the presence of a large calcium break (F00) and the low radio flux density. Indeed, it has been proposed (Giommi & Padovani 1994) that BL Lac objects discovered in radio and X-ray surveys are the two extremes of a single population differing by the frequency of the high-energy cutoff in their energy distribution which is related to the maximum energy of the synchrotron emitting electrons. Moreover, there is increasing evidence that the SED of BL Lac objects and flat spectrum radio quasars (blazars) can be unified in a spectral sequence determined by the total luminosity (Fossati et al. 1998; Ghisellini et al. 1998). The objects populating the low-

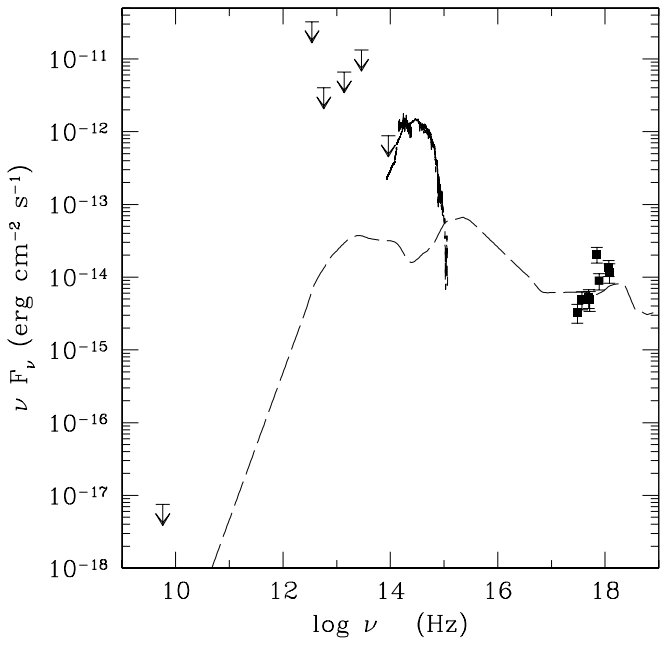

FIG. 4*a*

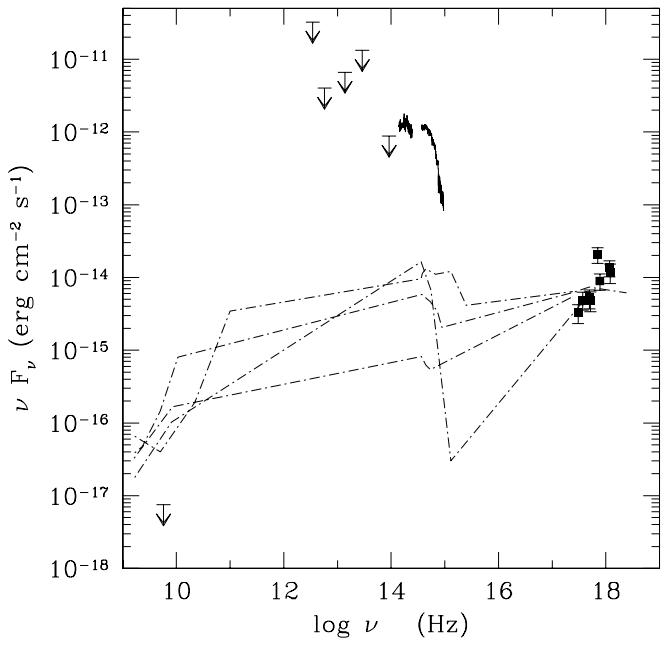

FIG. 4*b*

FIG. 4.—(*a*) Broadband SED of P3, including the upper limits in the 12 μm, 25 μm, 60 μm and 100 μm *IRAS* bands (retrieved from the NED database), is compared with the average SED of a radio-quiet AGN (*long dashed line*) plus an early-type galaxy template (*solid line*). (*b*) SED of the four low-luminosity AGNs in the Ho (1999) sample (*dot-dashed lines*) hosted by an E-galaxy (NGC 6251, NGC 4261, M84, and M87) normalized to the P3 X-ray flux.

luminosity extreme of the sequence peak at high frequency (in the X-ray band) and are called HBL. The upper limit on the 5 GHz radio luminosity ($<10^{39}$ ergs s^{-1}), on the radio to X-ray spectral index ($\alpha_{rx} < 0.6$, $F_\nu \propto \nu^{-\alpha}$), and the flat slope in the X-ray band would be consistent with the presence of a rather extreme member of the HBL class hosted by the P3 galaxy. The lack of X-ray variability, however, may constitute a problem with this interpretation.

An alternative explanation would be the presence of a hidden AGN. There are several examples of (obscured) AGNs discovered only by means of X-ray observations and not recognized as such by optical spectroscopy (see Matt 2001 and references therein). In order to test whether this is the case for P3, we have computed the expected optical magnitude in the R band assuming an average value of the optical–to–X-ray flux ratio typical of hard X-ray–selected unobscured quasars which turned out to be $R = 19.4$. For a standard Galactic extinction curve (Savage & Mathis 1979) the best-fit N_H value obtained from the analysis described in § 2.1 corresponds to $A_R = 2.6$. Extensive simulations have been carried out using the IRAF program ARTDATA to estimate whether or not a nuclear pointlike source with $R = 22$ would have been detected in the P3 nucleus. The results indicate that a nuclear source fainter than $R \approx 21.5$ could not be revealed with the quality of the present data which are limited by poor seeing conditions (about 1.″8). Although the present findings indicate that a mildly obscured AGN could be hosted by P3, we note that hard X-ray–selected objects with $L_X > 10^{42}$ ergs s^{-1} are generally characterized (with some exceptions; see, e.g., Brandt et al. 1997) by a dust-to-gas ratio much lower than the Galactic standard (Maiolino et al. 2001). Taking these results at the face value the putative X-ray mildly obscured nucleus would have probably been detected in the optical band, though this conclusion is subject to some uncertainties on the relation between X-ray and optical absorption.

As a final possibility, we have considered the hypothesis of a Compton-thick ($N_H \gtrsim 1.5 \times 10^{24}$ cm^{-2}) AGN. The P3 SED is compared (Fig. 5) with that of NGC 6240, a highly obscured AGN considered to be the prototype of this class of objects (Vignati et al. 1999). The NGC 6240 SED is normalized to match the P3 optical flux. Besides the disagreement in the radio band and at 60 μm, which could be due to a more intense star formation in NGC 6240, the P3 multiwavelength data are in relatively good agreement with the obscured AGN template. If P3 hosts a Compton-thick AGN with an SED similar to that of NGC 6240, then a luminous ($L_X \simeq 10^{44}$ ergs s^{-1}) X-ray source should be present at higher energies. In this case, the observed X-ray emission would be due to a scattered nuclear component known to be common among highly obscured AGN (Vignali et al. 2001 and references therein). The lack of strong X-ray variability would support this hypothesis.

Whatever is the nature of the AGN powering P3, it is interesting to see how a source with similar broadband properties would appear at high redshift and whether P3-like objects constitute a significant fraction of the X-ray faint sources that are being discovered in deep surveys (Alexander et al. 2001). The 2–10 keV P3 luminosity can be detected, at the limit of the present *Chandra* surveys, up to $z \simeq 1.5$. At this redshift, the optical and infrared magnitudes of a passively evolving elliptical galaxy (Pozzetti et al. 1998) would be $R \simeq 24.2$ and $K' \simeq 18.5$. Such an object would not belong to the optically faint X-ray source population investigated by Alexander et al. (2001), but rather to the class of extremely red objects (EROs; $R–K > 5$). This is not surprising since passively evolving elliptical galaxies have extremely red colors at $z > 1$. The EROs' X-ray properties have recently been investigated using the 1 Ms exposure in the *Chandra* Deep Field North (Alexander et al. 2002). The objects detected in the hard (2–8 keV) band have extremely flat spectral slopes and X-ray properties consistent with those expected from obscured AGNs. It is also worth noting that a high-z P3-like object would be bright enough in the optical band to allow spectroscopic observations at 8 m class telescopes. Optical and infrared observations of faint X-ray sources might thus uncover several examples of completely hidden high-redshift AGNs.

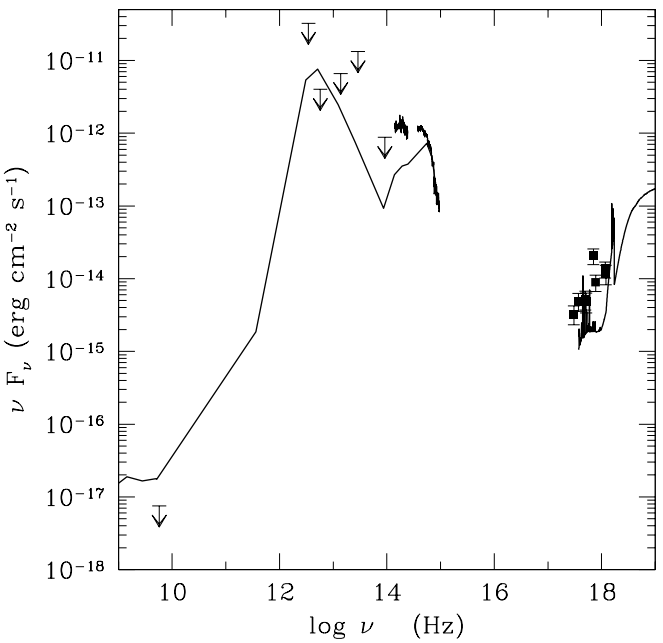

FIG. 5.—Observed SED is compared with that of the highly obscured Seyfert 2 galaxy NGC 6240.

4. CONCLUSIONS

The most important results obtained from our analysis of multiwavelength data can be summarized as follows.

1. The high X-ray luminosity and hard X-ray spectrum clearly indicate the presence of nuclear activity in P3.
2. There is no evidence of AGN emission lines in either the optical or infrared spectra.
3. The upper limit on the 5 GHz radio emission qualifies the AGN hosted by P3 (regardless of its origin) as a radio-quiet object.
4. The multiwavelength properties allow us to rule out ADAF emission and the presence of a low-luminosity AGN with an SED similar to those of the few nearby objects in the Ho (1999) sample.
5. An extreme BL Lac object, where the level of the non-thermal continuum in the radio and optical bands is very low, could provide an acceptable explanation of the P3 SED. The lack of X-ray variability, however, seems to be at odds with this interpretation.
6. The AGN responsible for the high X-ray luminosity is likely to be hidden by a substantial (possibly Compton thick) column of cold absorbing gas. If this is the case most

of the observed X-ray emission would be due to a scattered/reprocessed nuclear component.

7. Sensitive broadband observations of a sample of X-ray–bright, optically quiet galaxies are required to better understand their nature. Deep optical and infrared spectroscopy of X-ray–faint sources would allow us to assess their fraction in deep X-ray surveys, with important consequences for our understanding of the nature and the evolution of the X-ray background constituents.

We thank the entire *Chandra* team and the CXC team in particular for the support received in the data analysis. This research has made use of the NASA/IPAC Extragalactic Database (NED), which is operated by the Jet Propulsion Laboratory, California Institute of Technology, under contract with the National Aeronautics and Space Administration. This paper used observations collected at the Australian Telescope Compact Array (ATCA), which is founded by the Commonwealth of Australia for operation as a National Facility by CSIRO. The authors acknowledge partial support by the ASI contracts I/R/103/00 and I/R/107/00 and the MURST grant Cofin-00-02-36. C. V. also thanks the NASA LTSA grant NAG5-8107 for financial support. We also thank the referee for a fast and detailed report that improved the presentation of the results.

REFERENCES

Alexander, D. M., Brandt, W. N., Hornschemeier, A. E., Garmire, G. P., Schneider, D. P., Bauer, F. E., & Griffiths, R. E. 2001, AJ, 122, 2156
Alexander, D. M., Vignali, C., Bauer, F. E., Brandt, W. N., Hornschemeier, A. E., Garmire, G. P., & Schneider, D. P. 2002, AJ, 123, 1149
Allen, S. W., Di Matteo, T., & Fabian, A. C. 2000, MNRAS, 311, 493
Baldi, A., Molendi, S., Comastri, A., Fiore, F., Matt, G., & Vignali, C. 2002, ApJ, 564, 190
Barger, A. J., Cowie, L. L., Bautz, M. W., Brandt, W. N., Garmire, G. P., Hornschemeier, A. E., Ivison, R. J., & Owen, F. N. 2001, AJ, 122, 2177
Brandt, W. N., Fabian, A. C., Takahashi, K., Fujimoto, R., Yamashita, A., Inoue, H., & Ogasaka, Y. 1997, MNRAS, 290, 617
Brandt, W. N., et al. 2001, AJ, 122, 2810
Brandt, W. N., Laor, A., & Wills, B. J. 2000, ApJ, 528, 637
Devillard, N. 1998, Messenger, 87, 19
Dickey, J. M., & Lockman, F. J. 1990, ARA&A, 28, 215
Elvis, M., et al. 1994, ApJS, 95, 1
Fabbiano, G., Kim, D. W., & Trinchieri, G. 1992, ApJS, 80, 531
Fiore, F., et al. 2000, NewA, 5, 143 (F00)
Fossati, G., Maraschi, L., Celotti, A., Comastri, A., & Ghisellini, G. 1998, MNRAS, 299, 433
Freeman, P. E., Kashyap, V., Rosner, R., & Lamb, D. 2002, ApJS, 138, 185
Ghisellini, G., Celotti, A., Fossati, G., Maraschi, L., & Comastri, A. 1998, MNRAS, 301, 451
Giacconi, R., et al. 2001, ApJ, 551, 664
Giommi, P., & Padovani, P. 1994, MNRAS, 268, L51
Griffiths, R. E., Georgantopoulos, I., Boyle, B. J., Stewart, G. C., Shanks, T., & Della Ceca, R. 1995, MNRAS, 275, 77
Hamuy, M., et al. 1994, PASP, 106, 566
Ho, L. C. 1999, ApJ, 516, 672
Horne, K. 1986, PASP, 98, 609
Hornschemeier, A., et al. 2001, ApJ, 554, 742
Loewenstein, M., Mushotzky, R. F., Angelini, L., Arnaud, K. A., & Quataert, E. 2001, ApJ, 555, L21
Lumb, D. H., Guainazzi, M., & Gondoin, P. 2001, A&A, 376, 387
Maiolino, R., Marconi, A., Salvati, M., Risaliti, G., Severgnini, P., Oliva, E., La Franca, F., & Vanzi, L. 2001, A&A, 365, 28
Matt, G. 2001, in Issues in Unification of AGNs, ed. A. Marconi, R. Maiolino, & N. Nagar (San Francisco: ASP)
Moorwood, A. F. M., et al. 1999, Messenger, 95, 1
Mushotzky, R. F., Cowie, L. L., Barger, A. J., & Arnaud, K. A. 2000, Nature, 404, 459
Nandra, K., George, I. M., Mushotzky, R. F., Turner, T. J., & Yaqoob, T. 1997, ApJ, 476, 70
Patat, F. 1999 Efosc2 Users's Manual, LSO-MAN-ESO-36100-0004
Pozzetti, L., Madau, P., Zamorani, G., Ferguson, H. C., & Bruzual, A. G. 1998, MNRAS, 298, 1133
Quataert, E., & Narayan, R. 1999, ApJ, 520, 298
Savage, B. D., & Mathis, J. S. 1979, ARA&A, 17, 73
Schmidt, M., et al. 1998, A&A, 329, 495
Snowden, S. L. 2002, in New Visions of the X-Ray Universe in the *XMM-Newton* and *Chandra* Era (ESA SP-488; Noordwijk: ESA)
Tozzi, P., et al. 2001, ApJ, 562, 42
Van der Bliek, N. S., Manfroid, J., & Bouchet, P. 1996, A&AS, 119, 547
Vignali, C., Comastri, A., Fiore, F., & La Franca, F. 2001, A&A, 370, 900
Vignati, P., et al. 1999, A&A, 349, L57